RECEIVED BY TIC AUG 24 1978

LBL-7905

COMPUTER AIDED DESIGN OF SOLONOID MAGNETS

Juan M. DeOlivares
(M. E. thesis)

June 1978

Prepared for the U. S. Department of Energy
under Contract W-7405-ENG-48

COMPUTER AIDED DESIGN OF SOLENOID MAGNETS

Juan M. DeOlivares

Lawrence Berkeley Laboratory
University of California
Berkeley, California 94720

June 1978

ABSTRACT

Computer programs utilizing Legendre functions and elliptic integral functions have been written to aid in the design of solenoid magnets.

The field inside an axisymmetric magnet can be expanded in a converging power series of Legendre functions. The Legendre function approach is very useful for designing solenoid magnets with a high degree of field uniformity. This approach has been programed on the LBL CDC 7600 computer so that one can design an axisymmetric magnet which meets any desired field structure. This report presents two examples of computer designed solenoids.

A computer program utilizing elliptic integral functions was also written for the LBL CDC 7600 computer. This method was used in a computer program to verify the results obtained from the Legendre approach and for field calculations within the conductor.

The elliptic integral field calculations within the conductor showed that thin solenoids produce field peaking at the ends of the magnet. Computer data is generated for various magnet geometries and compared with theoretical predictions. Computer results and theoretical prediction both show that field peaking is reduced for longer coils, increased for

thinner coils and field peaking is a logarithmic function of length, thickness and radius.

Introduction

The vector potential and the field inside an axisymmetric magnet (solenoid) can be expanded in a converging power series of spherical functions or Legendre functions. The Legendre function approach is very useful for designing solenoid magnets with a high degree of field uniformity. This approach has been programmed on the LBL 7600 computer so that one can design an axisymmetric magnet configuration which meets any desired field structure.

The field inside a solenoid can also be calculated using elliptic integrals. This method was used in a computer program to verify the results obtained from the Legendre approach and for field calculations within the conductor.

The elliptic integral field calculations within the conductor showed that thin solenoids produce field peaking at the ends of the magnet.

Computer data is generated to determine how peaking is affected by magnet geometry. These results are compared with theoretical predictions.

Series expansion of the magnetic field of a circular loop of current using Legendre functions. (See Fig. 1)

One can show, using Maxwells equations, that there exists a magnetic vector potential which is related to the current density through Poisson's equation:

$$\nabla^2 \vec{A} = - \mu_o \vec{j}. \tag{1}$$

When the current density is equal to 0 the equation becomes:

$$\nabla^2 \vec{A} = 0. \tag{2}$$

This equation is extremely difficult to solve because of it's vector nature. Smythe presents a simplier method. He shows that $\vec{A}$ can be written as:[1]

$$\vec{A} = \nabla X \vec{W} \tag{3}$$

if

$$\nabla \cdot \vec{A} = 0. \tag{4}$$

$\vec{W}$ is a vector composed of two components each derivable from a scalar potential.

$$\vec{W} = \hat{u}\, W_1 + \hat{\mu} \times \nabla W_2 \tag{5}$$

where

$$\nabla^2 W_1 = \nabla^2 W_2 = 0 \tag{6}$$

and $\hat{\mu}$ is an arbitrary vector choosen so that:

$$\nabla^2 \vec{A} = \nabla X (\nabla^2 \vec{W}) = 0 \tag{7}$$

$\hat{u} = \hat{i},\hat{j},\hat{k}$ or $\hat{r}$ are suitable choices.

It can be shown that W_2 contributes nothing to $\vec{B}$ in the magnetostatic case. Therefore one can solve for $\vec{B}$ using only W_1, a scalar function.

$$\nabla^2 W_1 = 0. \tag{8}$$

One then uses $W = \hat{\mu}\ W_1$ and the expression $\vec{A} = \nabla X \vec{W}$ for $\vec{A}$. Using $\vec{B} = \nabla X \vec{A}$ one obtains $\vec{B}$ in terms of W_1.

$$\vec{B} = \nabla X (\nabla X \hat{\mu} W_1) \tag{9}$$

One solves for W_1 in terms of orthogonal expansions and can, therefore, obtain $\vec{B}$ in terms of orthogonal expansions.

In spherical polar coordinates, with $\vec{B}$ independent of ϕ, the components of $\vec{B}$ are given by:

$$Br = \frac{\partial^2 (rW_1)}{\partial r^2} \tag{10}$$

$$B_\theta = \frac{\partial^2 (rW_1)}{r \partial r \partial \theta} \tag{10a}$$

and

$$A_\phi = \frac{\partial W_1}{\partial \theta} . \tag{10b}$$

The solution of $\nabla^2 W_1 = 0$ in the case of no ϕ dependence is given by equation 11.

$$W_1 = [Ar^n + B r^{-(n+1)}] [C P_n (\cos \theta) + DQ_n (\cos \theta)] . \tag{11}$$

The solution $Q_n (\cos \theta)$ is rejected because $Q_n (0) \to \infty$.

W_1 must satisfy the following conditions:

- W_1 must be finite at $r = 0$ and $r = \infty$. Therefore the solution is divided into W_i for $r < r_c$ and W_o for $r > r_c$

$$W_i = Ar^n P_n (\cos \theta) \tag{12}$$

$$W_o = Br^{-(n+1)} P_n (\cos \theta) \tag{12a}$$

- $W_i = W_o$ at $r = r_c$ (12b)

- Equation 13 (Ampere's law) must be satisfied

$$\oint \vec{B} \cdot d\vec{\ell} = \mu_o i_\phi . \tag{13}$$

If we take a small loop around the current wire (see Fig. 2) then equation 13 becomes:

$$[(B\theta)_o - (B\theta)_i]\, r_c\, \Delta\theta = \mu_o\, i_\phi\, r_c\, \Delta\theta \tag{14}$$

i_ϕ is formed by expanding the stream function ψ in a series of Legendre functions.

$$\psi = \sum_{n=1}^{\infty} C_n P_n (\cos\theta) \tag{15}$$

where

$$i_\phi = \frac{1}{r_c} \frac{\partial\psi}{\partial\theta} \tag{16}$$

$$i_\phi = - \frac{1}{r_c} \sum_{n=1}^{\infty} C_n P_n^1 (\cos\theta) \tag{16a}$$

Using ψ and substituting W_i and W_o in equation 14 one obtains

$$\mu_o \psi = r_c \left[\frac{\partial W_o}{\partial r} - \frac{\partial W_i}{\partial r} \right] \tag{17}$$

W_o and W_i must take the following forms to satisfy both equations 12 and 17

$$W_o = \sum_{n=1}^{\infty} - \frac{\mu_o}{2n+1} C_n \left(\frac{r_c}{r}\right)^{n+1} P_n (\cos\theta) \tag{18}$$

$$W_i = \sum_{n=1}^{\infty} - \frac{\mu_o C_n}{2n+1} \left(\frac{r}{r_c}\right)^{n} P_n (\cos\theta). \tag{18a}$$

We can find C_n by using the orthogonal properties of Legendre functions and equation 16a.

Using eq. 16a

$$i_\phi = -\frac{1}{r_c}\sum_{n=1}^{\infty} C_n P_n^1(\cos\theta). \qquad (16a)$$

And taking the current density i_ϕ to be equal to zero except for A band of width ΔS at $\theta = \theta_c$ which is so narrow that $P_n^1(\cos\theta)$ has the constant value $P_n^1(\cos\theta_c)$ on it. C_n is found to be

$$C_n = -\frac{(2n+1)}{2n(n+1)} \sin^2\theta_c P_n^1(\cos\theta_c). \qquad (19)$$

From this we find that for a single current band at r_c and θ_c

$$A_\phi = \frac{\mu_o I \sin^2\theta_c \sin\theta}{2} \sum_{n=1}^{\infty} \frac{1}{n(n+1)} \left(\frac{r}{r_c}\right)^n P_n^1(\cos\theta_c) P_n^1(\cos\theta) \qquad (20)$$

$$B_r = \frac{\mu_o I \sin^2\theta_c}{2r_c} \sum_{n-1}^{\infty} \left(\frac{r}{r_c}\right)^{n-1} P_n^1(\cos\theta_c) P_n(\cos\theta) \qquad (20a)$$

$$B_\theta = \frac{\mu_o I \sin^2\theta_c \sin\theta}{2r_c} \sum_{n=1}^{\infty} \frac{1}{n} \left(\frac{r}{r_c}\right)^{n-1} P_n^1(\cos\theta_c) P_n^1(\cos\theta) \qquad (20b)$$

The above apply at $r \leq r_c$ at all values of n. A similar set of equations applies for all n when $r \geq r_c$. They are as follows:

$$A_\phi = \frac{\mu_o I}{2} \sin^2\theta_c \sin\theta \sum_{n=1}^{\infty} \frac{1}{n(n+1)} \left(\frac{r_c}{r}\right)^{n+1} P_n^1(\cos\theta_c) P_n^1(\cos\theta) \qquad (21)$$

$$B_r = \frac{\mu_o I}{2 r_c} \sin^2\theta_c \sin\theta \sum_{n=1}^{\infty} \left(\frac{r_c}{r}\right)^{n+2} P_n^1 (\cos\theta_c) P_n (\cos\theta) \qquad (21a)$$

$$B_\theta = \frac{\mu_o I}{2 r_c} \sin^2\theta_c \sin\theta \sum_{n=1}^{\infty} \frac{1}{n} \left(\frac{r_c}{r}\right)^{n+2} P_n^1 (\cos\theta_c) P_n^1 (\cos\theta) \qquad (21b)$$

A soleroid magnet can be divided into many current bands which are at various radii r_c and various angles θ_c. The field generated by such a magnet can be calculated by summing the fields generated by the individual currents. Reasonably accurate calculations (say to 1 part in 10^5) of the solenoid magnet field can be achieved by dividing the coil into a hundred parts. One can simplify the calculation of the solenoid field, if the magnet is symmetric about the $\theta = \pi/2$ plane as well as the axis ($\theta = o$ or $\theta = \pi$). The symmetrical solenoid case is discussed in the next section.

Before proceeding with the symmetrical air core magnet case, it is useful to look at the properties of Legendre functions of first order and first degree.

When n is odd, $$P_n^1(\cos\theta_c) = P_n^1(\cos[\pi-\theta_c]), \qquad (22)$$

and when n is even, $$P_n^1(\cos\theta_c) = - P_n^1(\cos[\pi-\theta_c]). \qquad (22a)$$

From equations 22 and 22a one can show that for a cylindrical solenoid with symmetry, when $r \geq r_c$,

$$A_\phi = \sum_{n=1}^{\infty} \frac{A_n}{n(n+1)} r^n \sin\theta \, P_n^1(\cos\theta), \tag{23}$$

$$B_r = \sum_{n=1}^{\infty} A_n r^{n-1} P_n(\cos\theta), \tag{23a}$$

$$B_\theta = \sum_{n=1}^{\infty} \frac{A_n}{n} r^{n-1} \sin\theta \, P_n^1(\cos\theta). \tag{23b}$$

When $r \geq r_c$,

$$A_\phi = \sum_{n=1}^{\infty} \frac{A_n^*}{n(n+1)} \left(\frac{1}{r}\right)^{n+1} \sin\theta \, P_n^1(\cos\theta), \tag{24}$$

$$B_r = \sum_{n=1}^{\infty} A_n^* \left(\frac{1}{r}\right)^{n+2} P_n(\cos\theta), \tag{24a}$$

$$B_\theta = \sum_{n=1}^{\infty} \frac{A_n^*}{n} \left(\frac{1}{r}\right)^{n+2} \sin\theta \, P_n^1(\cos\theta). \tag{24b}$$

where A_n and A_n^* are defined as follows:

$$A_n = \mu_o I \sin^2\theta_c \, P_n^1(\cos\theta_c) \left(\frac{1}{r_c}\right)^n \tag{25}$$

and

$$A_n^* = \mu_o I \sin^2\theta_c \, P_n^1(\cos\theta_c) \, r_c^{n+1} \tag{25a}$$

$$= A_n r_c^{2n+1} \tag{25b}$$

The A_n and A_n^* terms are defined by equations 25 and 25a. The values of A_n and A_n^* given by equations 25 and 25a do not apply for all values of n. When there is dipole symmetry, A_n and A_n^* are equal to zero for all even n. The odd values of A_n and A_n^* are given by equations 25 and 25a. When there is quadrupole symmetry, A_n and A_n^* are equal to zero for all odd n. The even values of A_n and A_n^* are given by equations 25 and 25a.

Symmetrical solenoid magnets without iron. Two kinds of symmetry will be described here. The first, which one may call dipole symmetry, has current of the same sign which are symmetrical about the $\theta = \pi/2$ plane (see Fig. 3a). The second kind of symmetry, which can be called quadrupole symmetry, has currents of opposite sign which are symmetrical about the $\theta = \pi/2$ plane (see Fig. 3b). This permits one to treat a current at $\theta = \theta_c$ along with a current at $\theta = \pi - \theta_c$. As a result, one can reduce the number of calculation steps by a factor of two or more.

Symmetrical solenoid magnets with iron. Expansion of the magnetic field with Legendre functions may be applied to solenoidal (axialsymmetric) magnets which have iron shields. One must assume that the permeability of the iron μ is infinite. (It should be noted that the real iron case $\mu \neq \infty$ can often be treated as a perturbation of the $\mu = \infty$ case.) Two kinds of iron poles are assumed here: (1) spherical iron, and (2) flat poles which are perpendicular to the magnet axis. In both cases, the method of images is employed in the calculations.

Before proceeding with the iron cases, it is useful to develop a more general power series expansion which can be applied inside the innermost coil of the solenoid (where r will always be less than r_c).

Symmetry is assumed to be used in the calculation. The series form for vector potential A_ϕ and induction B_r and B_θ is as follows:

$$A_\phi = \sum_{n=1}^{\infty} \frac{C_n}{n(n+1)} r^n \sin\theta \, P_n^1(\cos\theta), \tag{26}$$

$$B_r = \sum_{n=1}^{\infty} C_n r^{n-1} P_n(\cos\theta), \tag{26a}$$

$$B_\theta = \sum_{n=1}^{\infty} \frac{C_n}{n} r^{n-1} \sin\theta \, P_n^1(\cos\theta). \tag{26b}$$

Equations 26, 26a, and 26b can be used for symmetrical magnets of either type since the C_n component is a function of r_c, θ_c and I only. The C_n components can be divided into two parts as follows:

$$C_n = A_n + B_n. \tag{27}$$

There the A_n component is due to the coils alone and the B_n component is due to the image currents in the iron. The A_n terms are given by equation 25; the B_n terms will be given in this section.

The B_n terms in a symmetrical magnet behave in the same way as the A_n terms. When dipole symmetry is evoked, $B_n = 0$ when n is even; when quadrupole symmetry is evoked, $B_n = 0$ when n is odd. The B_n terms depend on the geometry of the iron shield. (The shield geometry affects the location of the image currents.) Two infinite μ iron geometries are of general interest; they are: (1) A spherical shield where the coil is inside a hollow iron sphere. (2) Two flat parallel pole pieces which lie parallel to the $\theta = \pi/2$ plane. The first geometry may be of

some interest even when the central induction of the solenoid exceeds 2 tesla. The latter geometry is reasonable model for the iron shields used in a solenoid which has a central induction of less than say 1.8 to 2.0 tesla.

(a) A spherical iron shield. This case has only one image current for each coil current. The image current radius $r_{ci} = R^2/r_c$ where R is the iron shield radius and r_c is the coil current radius. The image current angle θ_c is the same as the coil current angle θ_c. (See Fig.4.) Therefore, the B_n for the spherical iron is as follows:

$$B_n = \mu_o I \sin^2\theta_c P_n^1 (\cos\theta_c) \frac{r_c^n}{R^{2n}} . \qquad (28)$$

The use of a spherical iron shell is desirable when the central induction of the solenoid exceeds two tesla. The shield radius R can be adjusted so that the iron is not saturated. If the shield is allowed to saturate, the effects of symmetry will remain. Saturation will appear as perturbations to the B_n terms. The lowest perturbation term will appear first and the others will appear as the iron saturates. Some of the iron saturation perturbation terms can be controlled by shaping the outer boundary of the iron shield. Spherical iron shields should be usable even when the central induction of the solenoid approaches four tesla.

(b) Parallel iron pole pieces. The B_n term will consist of an infinite number of image currents. The first image current will be located the same distance inside the iron pole piece as the current is from the pole. An image current is located inside the opposite pole as

well. The image currents also form image currents in the poles (see Fig. 5). In general, the B_n term is a symmetrical magnet will take the following form:

$$B_n = \sum_{n=1}^{\infty} b_m \mu_o I \sin^2(\theta_{cm}) P_n^1(\cos\theta_{cm}) \left(\frac{1}{r_{cm}}\right)^n . \qquad (29)$$

The value of b_m depends on the symmetry used. $b_m = 1$ for all m when dipole symmetry applies. When quadrupole symmetry is used $b_m = +1$ when $m = 1, 4, 5, 8, 9, \cdots$ and $b_m = -1$ when $m = 2, 3, 6, 7, 10, 11, \cdots$.

θ_{cm} and r_{cm} take the following form when m is odd:

$$\theta_{cm} = \tan^{-1}\left(\frac{2r_c \sin\theta_c}{(m+1)L - 2r_c \cos\theta_c}\right) \qquad (30)$$

$$r_{cm} = \left[\left(\frac{(m+1)}{2} L - r_c \cos\theta_c\right)^2 + r_c^2 \sin^2\theta_c\right]^{1/2} . \qquad (30a)$$

When m is even:

$$\theta_{cm} = \tan^{-1}\left(\frac{2r_c \sin\theta_c}{mL - 2r_c \cos\theta_c}\right), \qquad (31)$$

$$r_{cm} = \left[\left(\frac{m}{2} L + r_c \cos\theta_c\right)^2 + r_c^2 \sin^2\theta_c\right]^{1/2} . \qquad (31a)$$

where θ_c is the coil current angle; r_c is the coil current radius (m); I is the magnitude of the current (A); L is the distance between the flat parallel iron pole pieces (m); and μ_o is the permeability of a vacuum.

The use of parallel poles is particularly desirable when the central induction of the solenoid is below the saturation induction of the iron. Saturation of the iron introduces field aberrations in which the lowest order term will be worst, followed by the next order term. If the solenoid has many evenly spaced coils, the infinite solenoid case is approximated. Using the parallel pole iron shield, one can get a field which is a good dipole type structure.

Newton-Raphson Method to Obtain Desired Coefficients

Summing the nth coefficient from each current loop, one obtains a total C_n for the magnet. If

$$C_n = C_n(G_1, G_2, \cdots G_k) \tag{32}$$

where G_n are magnet parameters, such as current, inner radius, length, etc. we can expand C_n in a Taylor series about the initial guess values for the parameters G_1^o through G_k^o. Neglecting higher order terms:

$$C_n(G_1, G_2, \cdots G_n) + \left.\frac{\partial C_n}{\partial G_1}\right|_{G_1^o} \Delta G_1 + \left.\frac{\partial C_n}{\partial G_2}\right|_{G_2^o} \Delta G_2 + \cdots \left.\frac{\partial C_n}{\partial G_k}\right|_{G_k^o} \Delta G_k$$

$$= C_n(G_1 + \Delta G_1,\ G_2 + \Delta G_2,\ \cdots G_k + \Delta G_k). \tag{33}$$

We would like ΔG_n's such that $C_n \to D_n$, where D_n are the desired values of the coefficients.

Therefore eq. 33 can be written as

$$D_n = C_n^o + \left.\frac{\partial C_n}{\partial G_1}\right|_{G_1^o} \Delta G_1 + \left.\frac{\partial C_n}{\partial G_2}\right|_{G_2^o} \Delta G_2 + \cdots \left.\frac{\partial C_n}{\partial G_k}\right|_{G_k^o} \Delta G_k \tag{34}$$

To solve for k coefficients one must solve k simultaneous equations as shown in eq. 35

$$\left.\frac{\partial C_1}{\partial G_1}\right|_{G_1^o} \Delta G_1 + \left.\frac{\partial C_1}{\partial G_2}\right|_{G_2^o} \Delta G_2 + \cdots \left.\frac{\partial C_1}{\partial G_k}\right|_{G_k^o} \Delta G_k = D_1 - C_1^o$$

$$\left.\frac{\partial C_2}{G_1}\right|_{G_1^o} \Delta G_1 + \left.\frac{\partial C_2}{G_2}\right|_{G_2^o} \Delta G_2 + \cdots \left.\frac{\partial C_2}{G_i}\right|_{G_k^o} \Delta G_k = D_2 - C_2^o$$

$$\vdots \qquad \vdots \qquad \vdots \qquad \vdots \qquad (35)$$

$$\left.\frac{\partial C_k}{\partial G_1}\right|_{G_1^o} \Delta G_1 + \left.\frac{\partial C_k}{\partial G_2}\right|_{G_2^o} \Delta G_2 + \cdots \left.\frac{\partial C_k}{\partial G_k}\right|_{G_k^o} \Delta G_k = D_k - C_k^o$$

Since $C_n(G_1, G_2, \cdots G_k)$ are generally non-linear an iterative solution is required.

In general, one would chose the lowest values of C_n because these would affect the magnetic field the most. For example, if the magnet is not to have symmetry, one would chose $C_1, C_2 \cdots C_k$ as the power series coefficients to tailor. If the magnet is to have dipole symmetry, C_1, C_3, $C_5 \cdots C_{2k-1}$ would be chosen. If the magnet is to have quadrupole symmetry, C_2, C_4, $C_6 \cdots C_{2k}$ would be chosen.

The preceding equations are solved for the correction function ΔG by matrix inversion. The correction functions are added to the G functions such that

$$G_{new} = G_{old} + \Delta G. \tag{36}$$

One calculates the various power series coefficients C_1, $C_2 \cdots C_k$ using the new values of G. The new values of C_1, $C_2 \cdots C_k$ are compared to D_1, $D_2 \cdots D_k$ on a term-by-term basis. If $D-C < \varepsilon$ (where ε is a small number like 10^{-6}) for all values of C and D from n = 1 to n = k, a solution has been found. If $D-C > \varepsilon$, derivatives of C with respect to the new values of G are taken and the simultaneous equations (Eq. 12) are solved so new values of G are found. Convergence, if there is convergence, will usually take less than ten iterations.

A lack of convergence is usually caused by the following: (1) there is no solution within the parameter boundary chosen which yields the desired magnetic structure, or, (2) the first guess was incorrectly chosen. Convergence may be obtained on solutions which may be correct mathematically, but they have no physical meaning. It may take several tries to find a current geometry which converges to a mathematically correct solution which has physical meaning.

Field of a Current Loop Using Elliptic Integrals

We assume here that eq. 1 applies

$$\nabla^2 \vec{A} = \mu_o \vec{J}. \tag{1}$$

If we have an arbitrary current carrying wire the solution of eq. 1 is given by eq. 37.

$$\vec{A} = \frac{\mu_o}{4\pi} \oint \frac{\vec{I} \cdot d\vec{s}}{r}. \tag{37}$$

For a current loop shown in Fig. 6, eq. 37 becomes

$$A_\phi = \frac{\mu_o a I}{\pi} \int_0^{\pi/2} \frac{(2 \sin^2\theta - 1) d\theta}{[(a+r_c)^2 + z_c^2 - 4ar_c \sin^2\theta]^{1/2}} \tag{38}$$

Rearranging equation 38, one obtains

$$A_\phi = \frac{\mu_o I}{\pi k} \left(\frac{r_c}{r}\right)^{1/2} [1 - \tfrac{1}{2} k^2) K - E]. \tag{39}$$

where K and E are elliptic integrals of the first and second kind.

$$K = \int_0^{\pi/2} [1 - k^2 \sin^2\phi]^{-1/2} \, d\phi \tag{40}$$

$$E = \int_0^{\pi/2} [1 - k^2 \sin^2\phi]^{1/2} \, d\phi \tag{40a}$$

and

$$k^2 = 4ar_c [(a + r_c)^2 + z_c^2]^{-1} \tag{40b}$$

Using $\vec{B} = \nabla \times \vec{A}$ one obtains the field components B_r and B_z show in eqs. 41 and 41a

$$B_r = \frac{\mu_o I}{2\pi} \frac{Z_c}{r_c[(a + r_c)^2 + Z_c^2]^{1/2}} \left[-K + \frac{a^2 + r_c^2 + Z_c^2}{(a - r_c)^2 + Z_c^2} E \right] \quad (41)$$

$$B_z = \frac{\mu_o I}{2\pi} \frac{}{[(a + r_c)^2 + Z_c^2]^{1.2}} \left[+K + \frac{a^2 - r_c^2 - Z_c^2}{(a - r_c)^2 + Z_c^2} E \right] \quad (41a)$$

Sample problems. The utility of the Legendre function power series technique is illustrated by the sample solutions given in this section. These problems are: (1) a uniform air core spherical solenoid and (2) correction coils for a solenoid with flat poles. Both of these problems could be encountered in the real world.

(a) Uniform field air core spherical solenoid. The uniform field air core spherical solenoid problem could be encountered in the field of solid state physics. Solenoid magnets have been built with a very uniform field within a small sphere located at the center of the magnet. Let us postulate a solenoid with the parameters given in Table 1. The spherical solenoid consists of three coil blocks in each half (see Fig. 7). The magnet coils have dipole symmetry. So, Cn for n = 2, 4, 6 ··· are eliminated by symmetry. There are five coil parameters available to zero five Cn coefficients. They are the five block angles G(2) through G(6) shown in Fig. 7. These five block angles can be set so that $Cn \approx 0$, for n = 3,5,7,9 and 11; and $Cn \neq 0$ when $n \geq 13$. Figure 7 shows the five

Table 1. Basic parameters for a uniform field air core solenoid magnet

Induction at center	3.0 tesla
Solenoid diameter	0.3 m
Solenoid length	0.3 m
Field quality within a sphere	10^{-6}
High quality field sphere diameter	0.1 m
Coil maximum thickness	0.01 m

coil parameters which are varied to eliminate C_3, C_5 $\cdots$ to C_{11}. A sixth parameter G(1), the current density in the coil blocks (which are all assumed to have the same current density), determines the induction of the magnet at its center (C_1 = 3.0 T). Table 2 shows the first guess and final value of each of the six magnet parameters. Table 3 shows a value of Cn at the surface of 0.1-m diameter sphere for each n between 1 and 20. The table shows the value for the first guess case and the final case. Table 4 shows a field map of the solenoid before optimization generated using the Legendre method. Table 5 shows the field map after optimization generated using the Legendre method. Table 6 is a field map of the optimized solenoid using the elliptic integral field expressions. Table 5 is in excellent agreement with Table 6.

As one moves further out towards the radius of the solenoid Table 5 and Table 6 differ slightly. This is to be expected since the series calculation converges slower at larger radius.

Table 2. The first guess and final value for each of the six parameters used to determine the design of a uniform solenoid.

	First Guess	Final Solution
G_1 The coil current density (Am^2)	3×10^8	3.514×10^8
G_2 2nd coil angle, Block 1 (deg.)	60.00	58.3490
G_3 1st coil angle, Block 2 (deg.)	50.00	55.1390
G_4 2nd coil angle, Block 2 (deg.)	45.00	39.2733
G_5 1st coil angle, Block 3 (deg.)	30.00	30.3888
G_6 2nd coil angle, Block 3 (deg.)	25.00	21.0544

Table 3. The numerical value of the C_n coefficients (units not given) at the surface of a sphere 0.1 m in diameter.

n	The C_n Value*	
	First Guess	Final Solution
1	2.25928	3.00000
3	-7.347×10^{-2}	-
5	-3.107×10^{-4}	-
7	2.987×10^{-4}	-
9	-5.671×10^{-6}	-
11	-1.929×10^{-6}	-
13	-2.036×10^{-8}	-1.849×10^{-6}
15	-2.036×10^{-8}	-1.756×10^{-7}
17	2.914×10^{-8}	2.276×10^{-8}
19	4.611×10^{-10}	2.886×10^{-9}

*Note Cn = 0 when n = 2, 4, 6....20....

Table 4. Field map of unoptimized spherical solenoid using Legendre functions.

FIELD MAP WITHOUT IRON

R COMPONENT OF B IN TESLA
THETA COMPONENT OF B IN TESLA

R (M) / T (RAD)	0.000	.006	.013	.019	.025	.031	.038	.044	.050
0.000	2.25928 0.00000	2.25813 0.00000	2.25469 0.00000	2.24894 0.00000	2.24090 0.00000	2.23055 0.00000	2.21790 0.00000	2.20298 0.00000	2.18578 0.00000
.314	2.14870 .69816	2.14787 .69753	2.14538 .69566	2.14122 .69253	2.13540 .68815	2.12791 .68251	2.11874 .67563	2.10791 .66750	2.09540 .65814
.628	1.82780 1.32797	1.82767 1.32720	1.82729 1.32490	1.82666 1.32107	1.82578 1.31570	1.82465 1.30879	1.82326 1.30033	1.82163 1.29033	1.81973 1.27875
.942	1.32797 1.82780	1.32840 1.82746	1.32969 1.82645	1.33184 1.82476	1.33485 1.82240	1.33872 1.81937	1.34346 1.81567	1.34908 1.81132	1.35559 1.80630
1.257	.69816 2.14870	.69860 2.14899	.69995 2.14984	.70218 2.15127	.70531 2.15327	.70932 2.15584	.71422 2.15899	.71999 2.16272	.72662 2.16704
1.571	-.00000 2.25928	-.00000 2.25985	-.00000 2.26158	-.00000 2.26444	-.00000 2.26846	-.00000 2.27361	-.00000 2.27989	-.00000 2.28730	-.00000 2.29581
1.885	-.69816 2.14870	-.69860 2.14899	-.69995 2.14984	-.70218 2.15127	-.70531 2.15327	-.70932 2.15584	-.71422 2.15899	-.71999 2.16272	-.72662 2.16704
2.199	-1.32797 1.82780	-1.32840 1.82746	-1.32969 1.82645	-1.33184 1.82476	-1.33485 1.82240	-1.33872 1.81937	-1.34346 1.81567	-1.34908 1.81132	-1.35559 1.80630
2.513	-1.82780 1.32797	-1.82767 1.32720	-1.82729 1.32490	-1.82666 1.32107	-1.82578 1.31570	-1.82465 1.30879	-1.82326 1.30033	-1.82163 1.29033	-1.81973 1.27875
2.827	-2.14870 .69816	-2.14787 .69753	-2.14538 .69566	-2.14122 .69253	-2.13540 .68815	-2.12791 .68251	-2.11874 .67563	-2.10791 .66750	-2.09540 .65814
3.142	-2.25928 -.00000	-2.25813 -.00000	-2.25469 -.00000	-2.24894 -.00000	-2.24090 -.00000	-2.23055 -.00000	-2.21790 -.00000	-2.20298 -.00000	-2.18578 -.00000

Table 5. Field map of optimized spherical solenoid using Legendre functions.

FIELD MAP WITHOUT IRON

R COMPONENT OF B IN TESLA
THETA COMPONENT OF B IN TESLA

R (M) / T (RAD)	0.000	.006	.013	.019	.025	.031	.038	.044	.050
0.000	3.00001 0.00000	3.00001 0.00000	3.00001 0.00000	3.00001 0.00000	3.00001 0.00000	3.00001 0.00000	3.00001 0.00000	3.00001 0.00000	3.00001 0.00000
.314	2.85318 .92705	2.85318 .92705	2.85318 .92705	2.85318 .92705	2.85318 .92705	2.85318 .92705	2.85318 .92705	2.85318 .92705	2.85318 .92705
.628	2.42706 1.76336	2.42706 1.76336	2.42706 1.76336	2.42706 1.76336	2.42706 1.76336	2.42706 1.76336	2.42706 1.76336	2.42706 1.76336	2.42706 1.76336
.942	1.76336 2.42706	1.76336 2.42706	1.76336 2.42706	1.76336 2.42706	1.76336 2.42706	1.76336 2.42706	1.76336 2.42706	1.76336 2.42706	1.76336 2.42706
1.257	.92705 2.85318	.92705 2.85318	.92705 2.85318	.92705 2.85318	.92705 2.85318	.92705 2.85318	.92705 2.85318	.92705 2.85318	.92705 2.85318
1.571	-.00000 3.00001	-.00000 3.00001	-.00000 3.00001	-.00000 3.00001	-.00000 3.00001	-.00000 3.00001	-.00000 3.00001	-.00000 3.00001	-.00000 3.00001
1.885	-.92705 2.85318	-.92705 2.85318	-.92705 2.85318	-.92705 2.85318	-.92705 2.85318	-.92705 2.85318	-.92705 2.85318	-.92705 2.85318	-.92705 2.85318
2.199	-1.76336 2.42706	-1.76336 2.42706	-1.76336 2.42706	-1.76336 2.42706	-1.76336 2.42706	-1.76336 2.42706	-1.76336 2.42706	-1.76336 2.42706	-1.76336 2.42706
2.513	-2.42706 1.76336	-2.42706 1.76336	-2.42706 1.76336	-2.42706 1.76336	-2.42706 1.76336	-2.42706 1.76336	-2.42706 1.76336	-2.42706 1.76336	-2.42706 1.76336
2.827	-2.85318 .92705	-2.85318 .92705	-2.85318 .92705	-2.85318 .92705	-2.85318 .92705	-2.85318 .92705	-2.85318 .92705	-2.85318 .92705	-2.85318 .92705
3.142	-3.00001 -.00000	-3.00001 -.00000	-3.00001 -.00000	-3.00001 -.00000	-3.00001 -.00000	-3.00001 -.00000	-3.00001 -.00000	-3.00001 -.00000	-3.00001 -.00000

Table 6. Field map of optimized spherical solenoid using elliptic integrals.

FIELD MAP WITHOUT IRON

R COMPONENT OF B IN TESLA
THETA COMPONENT OF B IN TESLA

R (M) / T (RAD)	.000	.006	.013	.019	.025	.031	.038	.044	.050
0.000	3.00001 .00000	3.00001 .00000	3.00001 .00000	3.00001 .00000	3.00001 .00000	3.00001 .00000	3.00001 -.00000	3.00001 -.00000	3.00001 -.00000
.314	2.85318 .92705	2.85318 .92705	2.85318 .92705	2.85318 .92705	2.85318 .92706	2.85318 .92706	2.85318 .92706	2.85318 .92706	2.85317 .92707
.628	2.42706 1.76336	2.42706 1.76336	2.42706 1.76336	2.42706 1.76336	2.42706 1.76336	2.42705 1.76337	2.42705 1.76337	2.42705 1.76337	2.42706 1.76335
.942	1.76336 2.42706	1.76336 2.42706	1.76336 2.42706	1.76336 2.42706	1.76336 2.42706	1.76336 2.42706	1.76335 2.42706	1.76335 2.42707	1.76333 2.42708
1.257	.92705 2.85318	.92705 2.85318	.92705 2.85318	.92705 2.85318	.92705 2.85318	.92705 2.85318	.92705 2.85318	.92705 2.85318	.92706 2.85318
1.571	-.00000 3.00001	-.00000 3.00001	-.00000 3.00001	-.00000 3.00001	-.00000 3.00001	-.00000 3.00001	-.00000 3.00001	-.00000 3.00001	-.00000 3.00001
1.885	-.92705 2.85318	-.92705 2.85318	-.92705 2.85318	-.92705 2.85318	-.92705 2.85318	-.92705 2.85318	-.92705 2.85318	-.92705 2.85318	-.92706 2.85318
2.199	-1.76336 2.42706	-1.76336 2.42706	-1.76336 2.42706	-1.76336 2.42706	-1.76336 2.42706	-1.76336 2.42706	-1.76335 2.42706	-1.76335 2.42707	-1.76333 2.42708
2.513	-2.42706 1.76336	-2.42706 1.76336	-2.42706 1.76336	-2.42706 1.76336	-2.42706 1.76336	-2.42705 1.76337	-2.42705 1.76337	-2.42705 1.76337	-2.42706 1.76335
2.827	-2.85318 .92705	-2.85318 .92705	-2.85318 .92705	-2.85318 .92705	-2.85318 .92706	-2.85318 .92706	-2.85318 .92706	-2.85318 .92706	-2.85317 .92707
3.142	-3.00001 .00000	-3.00001 .00000	-3.00001 .00000	-3.00001 .00000	-3.00001 .00000	-3.00001 .00000	-3.00001 -.00000	-3.00001 -.00000	-3.00001 -.00000

The solution given in Tables 2 and 3 can be obtained theoretically in a superconducting solenoid. It should be pointed out that real-life superconducting magnets have finite size winding errors. It might be possible to build a real magnet which has a field uniformity of 10^{-5} or better. It should be noted that diamagnetic current will cause large distortions in the field. As a result, field uniformities better than 10^{-4} may be difficult to obtain in real life without the use of special correction winding to get rid of the effects of residual field due to diamagnetic currents.

(b) Correction coils for a magnet with flat poles. Correction coils can be designed so that they produce Cn coefficients of a certain magnitude. There is a need for such correction coils in some of the solenoids now being designed for use in colliding beam experiments. These magnets have superconducting coils which are bounded at the ends by flat iron poles. The solenoid is supposed to produce a perfectly uniform field. Misalignment, saturation of the iron poles, and other effects may introduce errors in the field of a part or two in a thousand. Correction coils can remove 90 percent of these errors.

Figure 8 shows a system of eight coils which are to produce field corrections. The coils, depending how they are powered are supposed to produce C_1, C_2, C_3, C_4, C_5, C_6, and C_7 while eliminating all other Cn below n = 9. The eight coils are symmetrically placed on either side of the midplane, and evenly spaced between the iron poles ($\mu = \infty$) which are infinite planes (see Fig. 8). Table 7 gives the basic parameters of the correction coil blocks.

Table 7. Basic parameters of the correction coils

Correction coil spacing	0.4 m
Iron pole spacing	3.2 m
Correction coil radius	1.2 m
Value of Cn desired at surface of reference sphere	0.005 T
Radius of reference sphere	1.0 m

Symmetry is used to do the calculation. Dipole symmetry is used for C_1, C_3, C_5 and C_7 and quadrupole symmetry is used for C_2, C_4 and C_6. The parameter which one solves for is the current in each of the coils. There is a different current distribution in each of the coils for each correction Cn produced. The simultaneous equations generated by the computer are linear, so no iteration is required.

Table 8 shows current in each of the eight coils when the desired coefficient is produced. Table 9 shows the values of other coefficients when the desired one is produced.

A correction coil scheme similar to the one shown here is expected to be used on the TPC solenoid which is to be built in 1978. This magnet is supposed to produce a magnetic field which is good to a couple of parts in ten thousand. In the real TPC magnet, the iron poles are not infinite planes of infinite permeability. A technique such as this is expected to provide first order correction.

Table 8. The current in the eight correction coils when a desired multipole is generated on the surface of a 1.0 m radius reference sphere.

	Coil Current (A)						
	n = 1	n = 2	n = 3	n = 4	n = 5	n = 6	n = 7
Coil 1	1552	-6168	12192	-20912	27020	-34516	28208
Coil 2	1640	-488	-4244	13968	24208	38392	-34832
Coil 3	1572	-1464	-992	1376	312	-9372	11980
Coil 4	1596	-280	-2376	1764	1176	36	-2484
Coil 5	1596	280	-2376	-1376	1176	-36	-2484
Coil 6	1572	1464	-992	-1376	312	9372	11980
Coil 7	1640	488	-4244	-13968	24208	-38392	-34832
Coil 8	1552	6168	12192	20912	27020	34518	28208
Desired $C_n^* \rightarrow$	0.005	0.005	0.005	0.005	0.005	0.005	0.005

*On the surface of the reference sphere which is 1.0 meter in diameter

Table 9. The values of various C_n coefficients when the desired correction C_n is turned on.

	C_n Coefficient Value*						
n	$C_{nD} = 1$	$C_{nD} = 2$	$C_{nD} = 3$	$C_{nD} = 4$	$C_{nD} = 5$	$C_{nD} = 6$	$C_{nD} = 7$
1	0.00500	—	—	—	—	—	—
2	—	0.00500	—	—	—	—	—
3	—	—	0.00500	—	—	—	—
4	—	—	—	0.00500	—	—	—
5	—	—	—	—	0.00500	—	—
6	—	—	—	—	—	0.00500	—
7	—	—	—	—	—	—	0.00500
8	—	—	—	—	—	—	—
9	-0.00003	—	-0.00020	—	-0.00128	—	-0.00258
10	—	-0.00009	—	-0.00092	—	-0.00252	—
11	0.00009	—	-0.00020	—	0.00014	—	-0.00117
12	—	-0.00001	—	0.00064	—	0.00091	—
13	-0.00017	—	0.00039	—	0.00007	—	0.00174

*On the surface of a reference sphere 1.0 m in radius

Field Calculation Within the Conductor Using Elliptic Integrals

Once the parameters for a solenoid magnet with a desired field structure are determined, the field structure within the conducting current loops must be found in order to determine: (1) the forces on the magnet resulting from the magnetic-current interaction and for a super conducting magnet (2) the maximum current that can be applied which will not exceed the critical current and field for the superconducting wire. A typical critical field and current curves for superconductor are shown in Fig. 9.

The Legendre function field expressions are cumbersome to calculate conductor field because both $r > r_c$ and $r < r_c$ expressions must be used. The elliptic integral expressions are easier to use in that only one expression is needed. But symmetry cannot be invoked as with the Legendre approach to reduce the number of calculatoins.

The elliptic integral field computer program models the solenoid as a series of current loops. The method cannot be used to determine the self field of a current loop because the loops are modeled as point currents. The elliptic integral field expressions become infinite when both the field calculation point and current point concide. Modeling the current loops as point currents is valid because, given a current loop of finite diameter where the current density varies only in the radial direction within the conductor, the magnetic field outside the conductor is equal to the field resulting from a current point containing the total current flowing through conductor placed at the center of the real conductor. If the field calculation points lie only in the center of current loops the self field term is zero. The field from k current loops in the center of the ith current loop is given by equation 42,

$$B(\text{at the ith loop}) = \sum_{\substack{n=1 \\ n\neq i}}^{k} B\left(\begin{array}{c}\text{resulting from} \\ \text{nth loop}\end{array}\right) \qquad (42)$$

This method was used for field calculations of thin solenoid magnets such as the C coil and TPC magnet which are being developed and built at the LBL. Thin solenoids were found to have field peaking occuring at the ends. Typically a solenoid has field peaking occurring in the middle. Typical field variation is shown in Fig. 10a. A thin magnet with end peaking is shown in Fig. 10b.

In the next section computer generated data is used to determine how field peaking varies with geometric parameters of the magnet. These results are compared with theoretical predictions.

COMPUTER RESULTS

A magnet consisting of two layers of 430 turns each was modeled varying the following parameters: (see Fig. 11)

length of the coil	(ℓ)
radius of the coil	(R)
thickness	(ε)

The C coil was modeled as a base case.

C coil parameters:

ℓ(cm)	R(cm)	X(cm)	J(A/cm^2)
70.0	100.0	0.36	49143.0

$\ell/R = 0.70$ $\quad \ell/\varepsilon = 194.44$

Figure 12 shows $|B|$ in the inner layer as one moves out towards the end of the coil for various valves of ℓ/R. Figure 12 indicates that for a given value of ℓ/ε , end enhancement is reduced as ℓ/R becomes large. Figure 12 with $\ell/R = 20$, shows end enhancement reduced.

Figure 13 shows $|B|$ as $f(z)$ for various values of ℓ/ε. Enhancement is diminished by decreasing ℓ/ε (i.e., make the coil thicker).

The field in the outer layer follows a similar pattern. The peak field in the outer layer always appears less than the peak field in the inner layer.

$$\frac{B \text{ (peak outer layer)}}{B \text{ (peak inner layer)}} = 0.93 \text{ as an average value.}$$

COMPUTER AND THEORETICAL RESULTS

It should be noted that the theoretical results are based on:

1. A solenoid of continuous and uniform current density, where as the computer model uses discreet current loops.
2. Theoretical values of the peak field are calculated at the very end of the coil at $X = -\varepsilon/2$ and $X = 0$, whereas the computer model calculates the peak field in the center of the end wire at $X = \pm \varepsilon/4$.

For $\ell/R = 0.70$, the following functions were found from the computer data:

$$\underline{X = -\varepsilon/4}$$

$$\frac{B_r}{B_o} = 0.5725 + 0.0763 \ \ln \ell/\varepsilon \qquad (43)$$

$$\frac{\bar{B_z}}{B_o} = 0.20 \qquad (43a)$$

$\underline{X = + \varepsilon/4}$

$$\frac{B_r}{B_o} = 0.5565 + 0.0781 \ln \ell/\varepsilon \qquad (44)$$

$$\frac{\bar{B_z}}{B_o} = 0.007. \qquad (44a)$$

B_r and B_z are peak field components in the inner layer, and B_o is the field resulting from an infinite solenoid of the same thickness and current density.

Phillipe Eberhard derived the following formula[2] for a solenoid of uniform current density for the

limiting cases $\ell/R >> 1$

and $\ell/R << 1$

For $\ell/R >> 1$

$\underline{x = 0}$

$$\frac{B_r}{B_o} = 0.2817 + 0.1592 \ln \frac{R}{\varepsilon} \qquad (45)$$

$$\frac{B_z}{B_o} = 0.25 \qquad (45a)$$

$\underline{x = - \varepsilon/2}$

$$\frac{B_r}{B_o} = 0.1714 + 0.1592 \ln \frac{R}{\varepsilon} \qquad (46)$$

$$\frac{B_z}{B_o} = 0.50 \qquad (46a)$$

For $\ell/R << 1$

$\underline{x = 0}$

$$\frac{B_r}{B_o} = 0.2695 + 0.1592 \ln \ell/\varepsilon \qquad (47)$$

$$\frac{B_z}{B_o} = 0. \qquad (47a)$$

$$\underline{x = -\ell/2} \qquad \frac{B_r}{B_o} = 0.1592 + 0.1592 \ln \ell/\epsilon \tag{48}$$

$$\frac{B_z}{B_o} = 0.25 \tag{48a}$$

The important features of the theory are:

a. logarithmic dependence on geometry

b. radius dominated function for $\ell/R \gg 1$

c. length dominated function for $\ell/R \ll 1$.

Tables 10-12 compare theoretical and computer generated values of B_r/B_o. Table 10 indicates that for $\ell/R < 1$, the computer data approaches theoretical values as $\ell/R \to 0$. But, Table 12 suggests that theoretical and computer data converge slower for different values of ℓ/ϵ. For example, at $\ell/R = 0.18$ and $\ell/\epsilon = 48.61$ instead of 194.44 as in Table 10, percent difference between theoretical and computer results is 12.5% instead of 0.3%. Data in Table 12 also indicates that, for a given value of ℓ/R, there is better agreement between theoretical and computer data for larger values of ℓ/ϵ.

Table 12 compares computer data and theoretical predictions for $\ell/R > 1$. There is insufficient consistent data to conclude whether or not computer data approaches the theoretical predictions as ℓ/R becomes large. The data does suggest that for a given value of ℓ/R, better agreement is obtained for smaller values of R/ϵ.

It is clear that these comparisons only apply for cases where a solenoid consists of two 430 turn layers. Changing the number of turns or layers may change these results.

Table 10.

ℓ/ε = 194.44 ℓ/R	THEORY B_r/B_o $(x = -\frac{\varepsilon}{2})$	COMPUTER DATA B_r/B_o $(x = -\frac{\varepsilon}{4})$	% Difference
0.70	0.998	0.968	3.0
0.35	0.998	0.986	1.2
0.18	0.998	0.995	0.3
0.01	0.998	0.997	0.1

Table 11.

		$\ell/R < 1$		
ℓ/R	ℓ/ε	COMPUTER DATA B_r/B_o $(x = -\frac{\varepsilon}{4})$	THEORY B_r/B_o $(x = -\frac{\varepsilon}{2})$	% Difference
0.70	12.15	0.757	0.557	26.4
0.70	24.31	0.811	0.667	17.8
0.70	48.61	0.865	0.778	10.1
0.70	97.22	0.919	0.888	3.4
0.70	194.44	0.968	0.998	3.1
0.35	97.22	0.934	0.888	4.9
0.35	194.44	0.986	0.998	1.2
0.18	43.61	0.890	0.778	12.6
0.18	51.47	0.901	0.787	12.7
0.18	194.44	0.995	0.998	0.30
0.01	194.44	0.997	0.998	0.10
0.01	194.44	0.997	0.998	0.10

Table 12

$\ell/R > 1$

ℓ/R	R/ε	COMPUTER DATA B_r/B_o $(x = \frac{\varepsilon}{4})$	THEORY B_r/B_o $(x = -\frac{\varepsilon}{2})$	% Difference
1.1	486.11	0.986	1.16	17.6
1.3	416.67	0.973	1.13	16.0
1.4	277.78	0.957	1.07	11.8
1.4	138.89	0.918	0.960	4.6
2.8	69.44	0.840	0.85	1.0
10.0	55.56	0.578	0.81	40.0
26.0	9.72	0.545	0.53	3.0
100.0	1.94	0.321	0.28	13.0

The following trends are substantiated by the theory and computer results:

1. For a given value of ℓ/ε, field enhancement is reduced as ℓ/R becomes larger (i.e., a longer coil),
2. Enchancement is a logarithmic function of geometric parameters, and
3. For a given value of ℓ/R, enhancement is increased as ε becomes small (thin coils).

Conclusion

This report has shown how Legendre functions can be utilized in a computer program to design a solenoid magnet with a desired field structure.

An elliptic integral computer field program can also be used to determine field structure within conducting areas. This information can then be used to determine structural support requirements and operating limits for thin superconducting magnets.

This work was done with support from the U.S. Department of Energy.

REFERENCES

1. W. R. Smythe, Static and Dynamic Electricity, McGraw Hill Book Co., New York, 1950.

2. Private communication with Phillipe Eberhard LBL Physics Division, March 1978.

3. The Design of Solenoid Magnets Using Legendre Functions, M. A. Green and J. M. DeOlivares, August 1977, LBL-6716

ACKNOWLEDGEMENTS

I wish to thank the Lawrence Berkeley Laboratory and the Mechanical Department for giving me the opportunity to perform this work. I would particularly like to thank Mike Green for his guidance, patience and encouragement.

FIGURE CAPTIONS

Fig. 1. A simple current loop is spherical coordinate form.

Fig. 2. Small loop around circular current wire.

Fig. 3. Symmetrical magnet structures with two current loops.

Fig. 4. A spherical iron shield around a symmetrical magnet (dipole symmetry) showing image currents.

Fig. 5. A symmetrical magnet (dipole symmetry) with flat iron poles.

Fig. 6. A simple axisymmetric current loop showing the direction of the current, vector potential and the components of induction.

Fig. 7. A good field quality spherical solenoid.

Fig. 8. A correction coil problem.

Fig. 9. Critical current vs critical field.

Fig. 10. Field variation in conductor of solenoids.

Fig. 11. Coil parameters.

Fig. 12. $|B|$ variation in conductor of solenoids for different values of ℓ/R.

Fig. 13. $|B|$ variation in conductor of solenoids for different values of ℓ/ε.

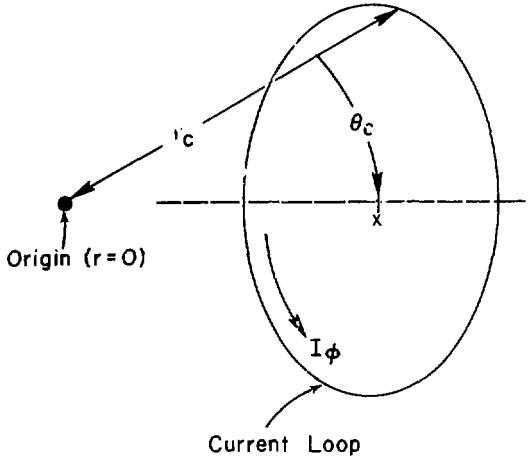

Fig. 1 XBL 778 9862

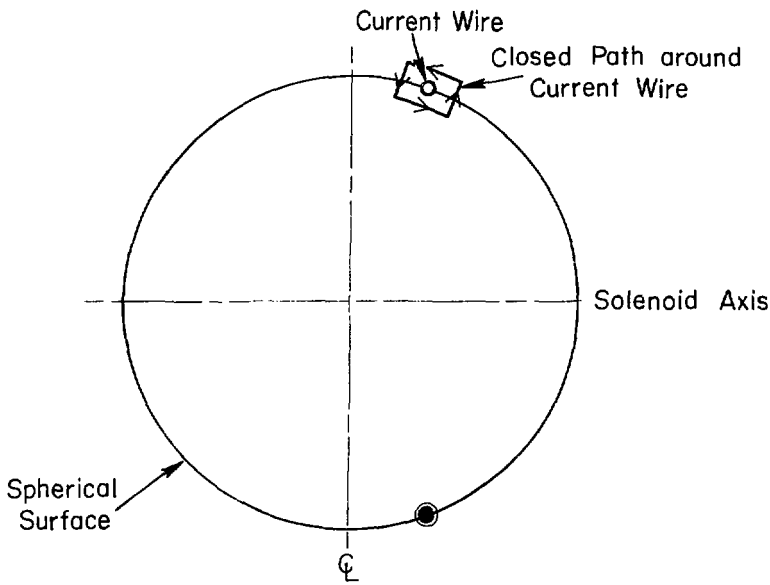

Fig. 2

XBL 786-9170

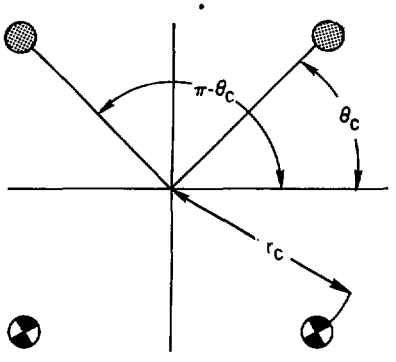

a) Dipole Symmetry (both currents have the same direction)

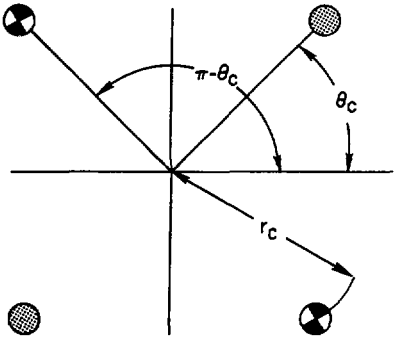

b) Quadrupole Symmetry (currents have opposite direction)

Fig. 3 XBL 778 9859

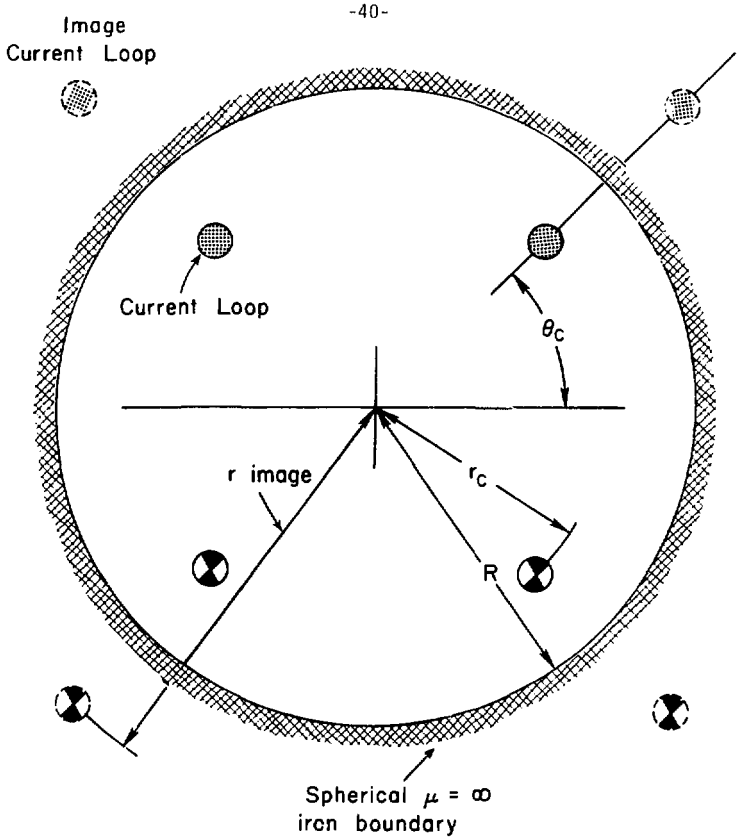

Fig. 4

XBL 778 9860

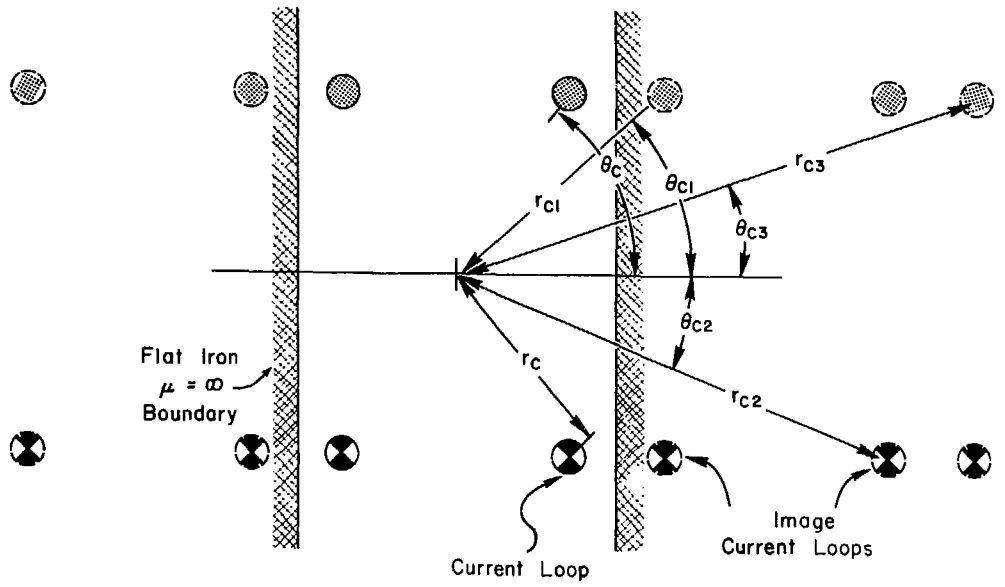

Fig. 5

XBL 778 9861

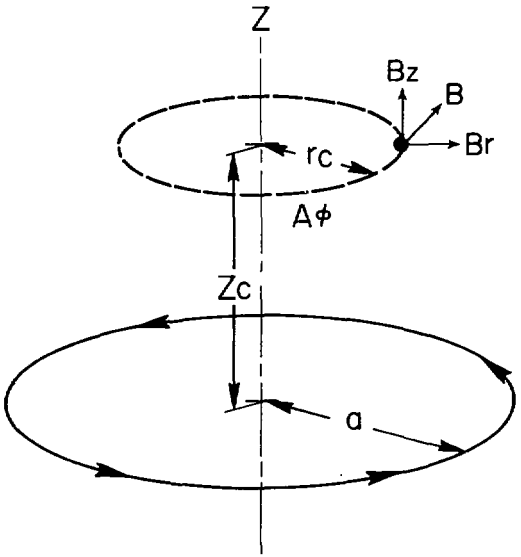

Current Loop of Current I

Fig. 6

XBL 785-9005

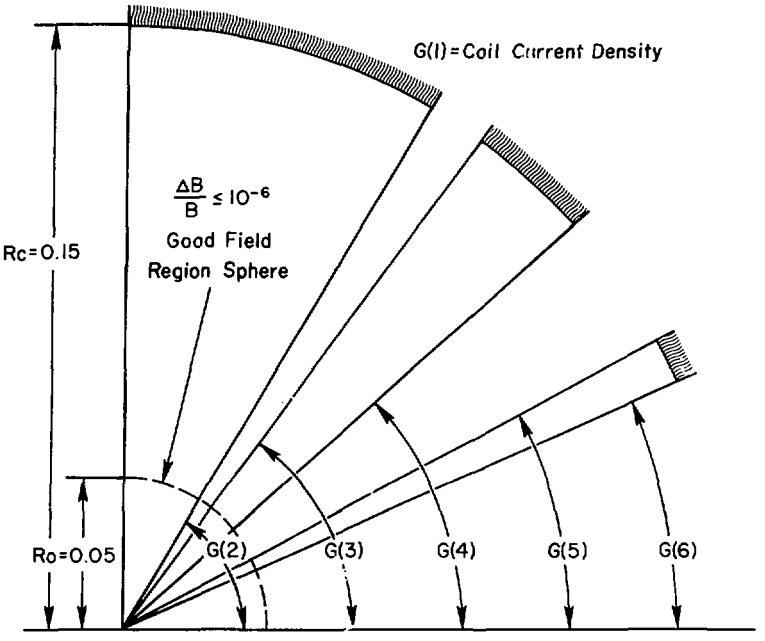

Good Field Quality Spherical Solenoid

XBL 778 9946

Fig. 7

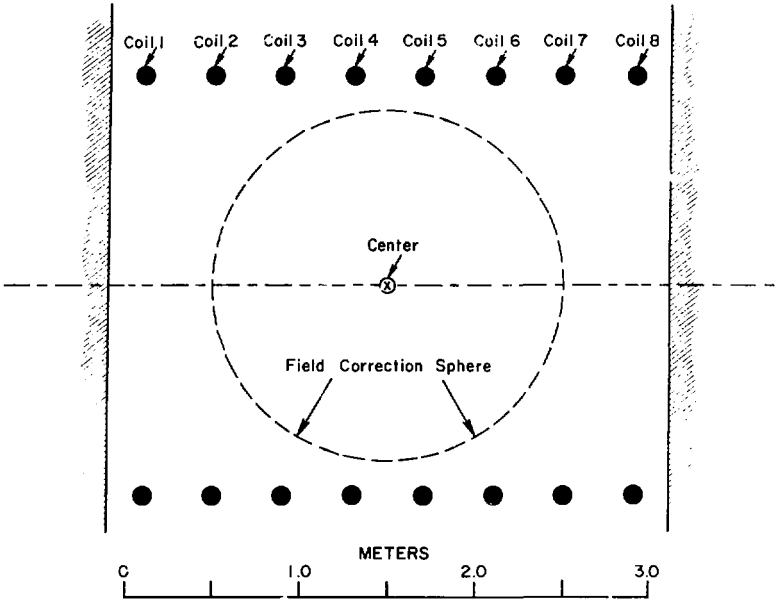

Correction Coil Problem

XBL 778 9947

Fig. 8

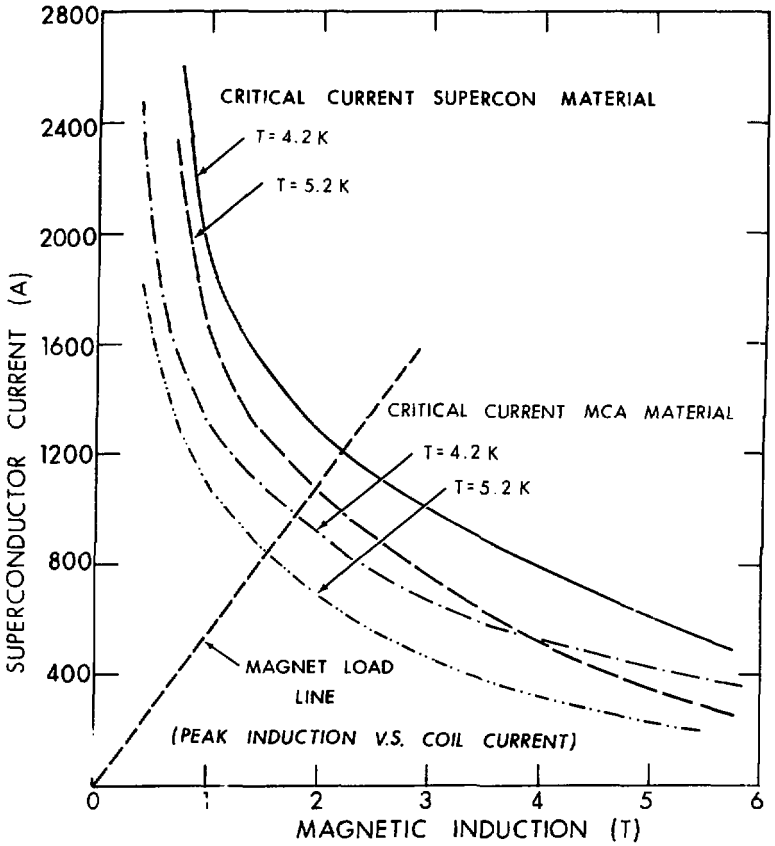

Fig. 9

XBL 774-8444

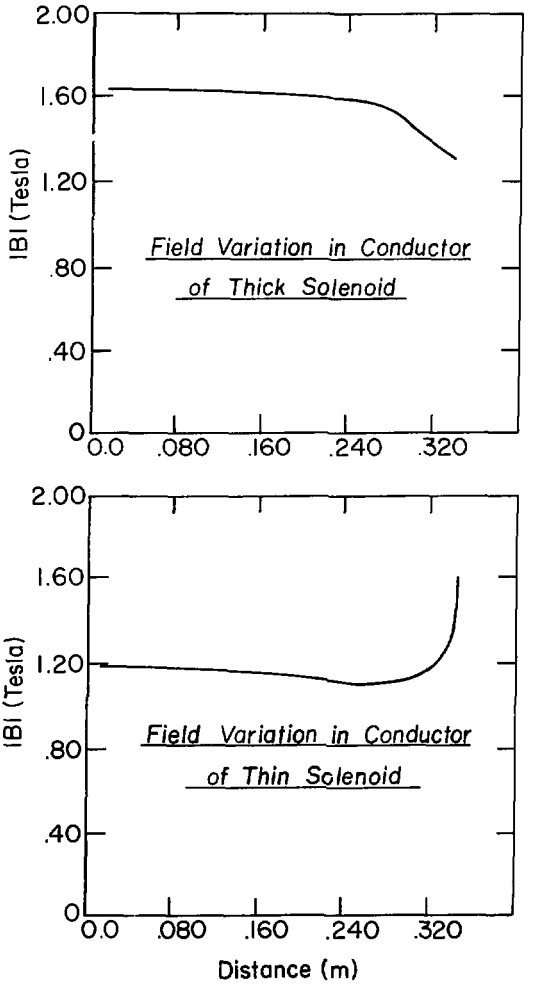

Fig. 19 XBL 786-9169

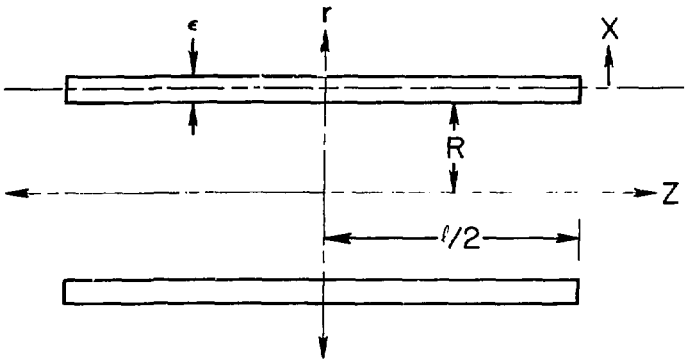

ℓ Length of the coil
R Radius of the coil
ϵ Thickness of the coil

Fig. 11

XBL 785-9007

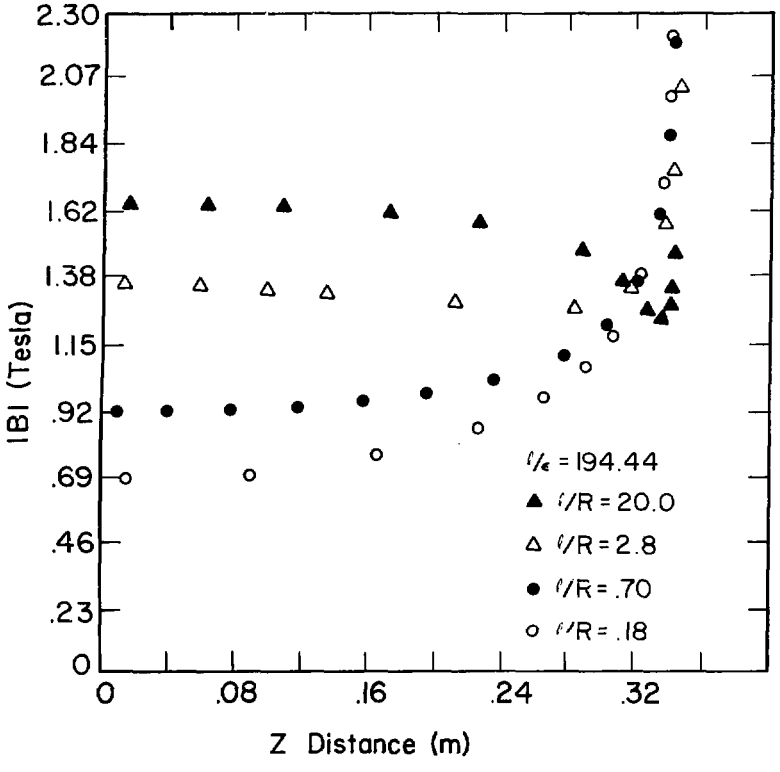

Fig. 12

XBL 785-9006

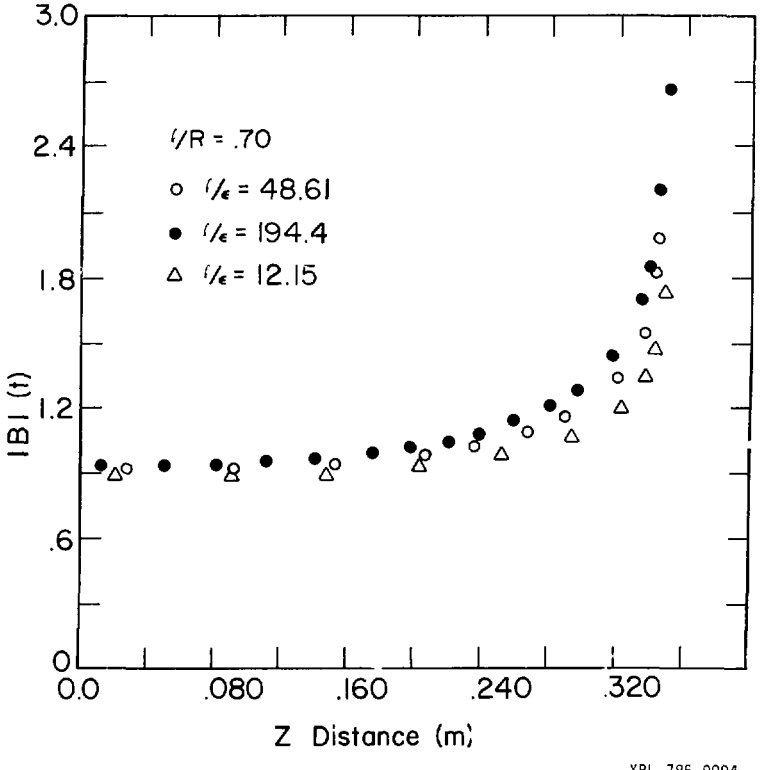

Fig. 13

XBL 785-9004